HHS Public Access

Author manuscript

Obesity (Silver Spring). Author manuscript; available in PMC 2024 July 01.

Published in final edited form as:

Obesity (Silver Spring). 2023 July ; 31(7): 1825–1843. doi:10.1002/oby.23774.

Pharmacological antagonism of receptor for advanced glycation end products signaling promotes thermogenesis, healthful body mass and composition, and metabolism in mice

Robin A. Wilson[1], **Lakshmi Arivazhagan**[1], **Henry H. Ruiz**[1], **Boyan Zhou**[2], **Kun Qian**[2], **Michaele B. Manigrasso**[1], **Rollanda Bernadin**[1], **Kaamashri Mangar**[1], **Alexander Shekhtman**[3], **Huilin Li**[2], **Ravichandran Ramasamy**[1], **Ann Marie Schmidt**[1]

[1]Diabetes Research Program, Department of Medicine, New York University Grossman School of Medicine, New York, New York, USA

[2]Departments of Population Health (Biostatistics) and Environmental Medicine, New York University Grossman School of Medicine, New York, New York, USA

[3]Department of Chemistry, State University of New York, Albany, New York, USA

Abstract

Objective: Optimal body mass and composition as well as metabolic fitness require tightly regulated and interconnected mechanisms across tissues. Disturbances in these regulatory networks tip the balance between metabolic health versus overweight and obesity and their complications. The authors previously demonstrated roles for the receptor for advanced glycation end products (RAGE) in obesity, as global- or adipocyte-specific deletion of *Ager* (the gene encoding RAGE) protected mice from high-fat diet-induced obesity and metabolic dysfunction.

Methods: To explore translational strategies evoked by these observations, a small molecule antagonist of RAGE signaling, RAGE229, was administered to lean mice and mice with obesity undergoing diet-induced weight loss. Body mass and composition and whole body and adipose tissue metabolism were examined.

Correspondence: Ann Marie Schmidt, Diabetes Research Program, Department of Medicine, New York University Grossman School of Medicine, Science Bldg., Room 615, 435 E. 30 St., New York, NY 10016, USA. annmarie.schmidt@nyulangone.org.

AUTHOR CONTRIBUTIONS

Robin A. Wilson designed the research, performed experiments, analyzed data, and wrote and edited the manuscript. Lakshmi Arivazhagan, Michaele B. Manigrasso, Rollanda Bernadin, and Kaamashri Mangar performed experiments and edited the manuscript. Boyan Zhou, Kun Qian, and Huilin Li performed data and statistical analyses and edited the manuscript. Lakshmi Arivazhagan, Henry H. Ruiz, Ravichandran Ramasamy, and Alexander Shekhtman contributed analytically and intellectually to the interpretation of data and edited the manuscript. Ann Marie Schmidt conceived studies, designed the research, supervised the design and completion of experiments, analyzed data, and wrote and edited the final manuscript.

CONFLICT OF INTEREST STATEMENT

Michaele B. Manigrasso, Ravichandran Ramasamy, Alexander Shekhtman, and Ann Marie Schmidt have patents and patent applications through New York University Grossman School of Medicine that have been submitted/published that are related to the work detailed in this manuscript. The other authors declared no conflict of interest.

SUPPORTING INFORMATION

Additional supporting information can be found online in the Supporting Information section at the end of this article.

Results: This study demonstrates that antagonism of RAGE signaling reduced body mass and adiposity and improved glucose, insulin, and lipid metabolism in lean male and female mice and in male mice with obesity undergoing weight loss. In adipose tissue and in human and mouse adipocytes, RAGE229 enhanced phosphorylation of protein kinase A substrates, which augmented lipolysis, mitochondrial function, and thermogenic programs.

Conclusions: Pharmacological antagonism of RAGE signaling is a potent strategy to optimize healthful body mass and composition and metabolic fitness.

INTRODUCTION

The regulation of energy intake, use, and storage requires exquisite coordination to prevent dysregulation of body mass and composition and metabolism. Overweight and obesity ensue because of endogenous and exogenous factors that thwart these programs. In this context, advanced glycation end products (AGEs) are formed during normal metabolism and aging [1, 2] and to excess during obesity and hyperglycemia [3]. The processing of foods at high temperatures also stimulates the formation of AGEs, which are not metabolically innocuous [4].

Interaction of AGEs with the multiligand receptor for advanced glycation end products (RAGE) induces various cellular pathways to impact metabolic and inflammatory diseases [5]. In humans without diabetes and with obesity versus the lean state, the accumulation of RAGE ligand carboxymethyllysine-AGE and RAGE expression are increased in subcutaneous adipose tissue (SAT) [6]. AGEs accumulate in the metabolic tissues of mice fed a high-fat diet (HFD; 60% of kilocalories from fat) [7]. RAGE is implicated in obesity, as protection from HFD-induced obesity and associated impaired glucose and insulin metabolism has been observed in mice bearing global or adipocyte-specific deletion of *Ager* (the gene encoding RAGE) [7–10] through upregulation of thermogenesis in interscapular brown adipose tissue (iBAT) and subcutaneous inguinal white adipose tissue (iWAT).

RAGE ligands bind at multiple sites on RAGE's extracellular domains [11, 12], suggesting that approaches targeting these domains might not be fully effective. The cytoplasmic domain of RAGE, required for RAGE signaling, binds to protein diaphanous homolog 1 (DIAPH1); silencing of *Diaph1* in cultured cells has been shown to suppress RAGE signaling [13, 14]. We earlier screened a small molecule library and identified molecules that reduced RAGE–DIAPH1 interaction and RAGE signaling [15]. Structure-activity relationship refinements led to the discovery of the chemical probe, RAGE229, *N*-(4-(7-cyano-4-(morpholin-4ylmethyl)quinolin-2-yl)phenyl)acetamide; *in vivo*, RAGE229 significantly reduced complications in mice with type 1-like or type 2-like diabetes [16].

We tested the hypothesis that pharmacological antagonism of RAGE signaling improves metabolic health in mice. We demonstrate that, in lean mice and mice with obesity undergoing diet-induced weight loss, administration of RAGE229 reduced body mass and adiposity and improved glucose, insulin, and lipid metabolism. In mouse and human adipocytes, RAGE229 bolstered phosphorylation of key cAMP-dependent protein kinase A (PKA) substrates and enhanced thermogenesis, lipolysis, and mitochondrial function.

METHODS

Animals, diets, and study approvals

All animal experiments were performed according to the NIH Guide for the Care and Use of Laboratory Animals and all protocols were approved by the Institutional Animal Care and Use Committee at New York University Grossman School of Medicine.

Six-week-old male or female mice (C57BL/6J) acquired from The Jackson Laboratory were randomly housed in groups (up to five per cage) and maintained on 5053-LabDiet. This diet is referred to as base diet. Mice were kept under a 12:12-hour (lights on at 6:30) light–dark photoperiod with ad libitum access to food and water unless otherwise specified for the pair feeding or other studies. Body weight was monitored on a biweekly basis unless otherwise noted in the specific experiments. When mice reached 26 weeks of age, mice were weight-matched and randomly allocated into two groups by a laboratory team member not involved in the study design or execution. Mice were separated by sex with two to three animals per cage. Of these groups, one set of mice was randomly assigned to remain on base diet described above, and the other set of mice was switched to RAGE229 diet (150 parts per million [ppm], approximately 30 mg/kg/d or 50 ppm, approximately 10 mg/kg/d; Envigo, Madison, Wisconsin). RAGE229 was added directly to base diet as powder (150 or 50 ppm, as indicated), and both diets were handled identically; the mix was pelleted and then subjected to irradiation prior to shipment. The stability and efficacy of the diet were previously extensively tested and reported [16].

In distinct studies, 6-week-old male mice (C57BL/6J) were purchased from The Jackson Laboratory and, on arrival, were randomly housed in groups (up to five per cage). Mice were maintained on the described base diet (5053-LabDiet), and acclimatized to the housing for 2 weeks. Mice were kept under a 12:12-hour (lights on at 6:30) light–dark photoperiod with ad libitum access to food and water unless otherwise specified for pair-feeding studies. From age 8 weeks, all mice were fed an HFD (60% calories from fat, D12492i; Research Diets, Inc., New Brunswick, New Jersey) to establish obesity, and body weight was monitored on a biweekly basis.

In all cases, mice were first fed the indicated base diet or the HFD. Then, immediately before the diet switch, mice were randomly assigned into two weight-matched groups; these two groups were then randomly assigned to be switched to either the RAGE229-containing diet or to base diet by a laboratory member not involved in the specific experimental design or the study execution.

Furthermore, in all experiments, mice undergoing the diet switch were adapted to the new diet by introducing a mixture of the previous diet (base diet or HFD) and post-switch diet (RAGE229 or base diet) in increasing proportions of the new diet such that mice were fully acclimated to the new diet over a period of 6 days.

Indirect calorimetry

At indicated time points, mice were individually housed in gas calibrated metabolic chambers (TSE Systems, Inc.) for 48 hours to measure the rate of oxygen consumption

(VO_2), carbon dioxide production (VCO_2), caloric intake, and physical activity and to determine energy expenditure through indirect calorimetry analyses. For the last 24 hours, energy expenditure, VO_2, and VCO_2 data were presented as line graphs and averaged to present as dot plots. Caloric intake and physical activity over the last 24 hours were added cumulatively and presented as line graphs and also totaled over 24 hours and presented as dot plots. Energy expenditure data were also analyzed using ANCOVA with body mass as covariate.

Mouse and human cell culture and RAGE229 treatment

C3H10T1/2 cells (ATCC-CCL-226) were cultured in complete media consisting of DMEM (ThermoFisher Scientific 11995065) containing 10% (volume per volume, vol/vol) fetal bovine serum (FBS) (Corning 35-010-CV) and 1% (v/v) penicillin–streptomycin, until 80% confluence. Cells were then differentiated for 5 days in DMEM containing 10% (vol/vol) FBS, 1 mg/mL of insulin (Sigma I6634), 2nM triiodothyronine (T3) (Sigma T2752), 0.5mM 3-isobutyl-1-methylxanthine (IBMX) (Sigma I5879), 1mM dexamethasone (Sigma D4902), 1mM rosiglitazone (Sigma R2408), and 1% (vol/vol) penicillin–streptomycin. Differentiated adipocytes were maintained for 2 days in DMEM supplemented with 10% (vol/vol) FBS, 1% (vol/vol) penicillin–streptomycin, insulin (1 mg/mL), and T3 (2 nM). Human subcutaneous primary adipocytes (deidentified White female, BMI = 20.6, age = 34 years) were procured from Cell Applications (S802s-05a, Lot#1687). Preadipocytes were cultured in preadipocyte growth medium (Cell Applications 811–500) until 100% confluence and differentiated to adipocytes in adipocyte differentiation medium (Cell Applications 811D-250) for 12 to 13 days.

Once adipocytes were fully differentiated, media was removed and replaced with complete media (for mouse adipocytes) or preadipocyte growth medium (for human adipocytes) supplemented with either RAGE229–100 μM (dissolved in dimethylsulfoxide [DMSO] or vehicle (equal concentrations of DMSO) for 12 hours, after which media was removed and cells were washed with phosphate-buffered saline (PBS) and then lysed to extract proteins.

Statistical analysis

Statistical analysis was performed using R version 3.6.3 and GraphPad Prism. Data were presented as mean ± SEM, except the epididymal white adipose tissue (eWAT) and iWAT area, for which median with 95% confidence intervals was presented. A linear mixed-effect model was adopted for correlated/time-series data with post hoc *t* test for group comparisons at each time point. For analysis of absolute body mass over indicated time periods, a piecewise linear mixed-effect model was fitted, with node set at 26 weeks, and difference was tested between body mass of the weight of base diet and RAGE229–150 or 50 ppm diet groups after the diet switch. For group comparisons, Shapiro–Wilk normality test was conducted first to establish normality for each group with prespecified significance level of 0.1, and, if normality test was passed, ANOVA or t test was used. If normality was not established, nonparametric Kruskal-Wallis test/Wilcoxon rank sum test was used. ANCOVA was used to test the effects of RAGE229 diet on energy expenditure variables, controlling for the effects of body mass. Finally, mediation analysis was performed using R package lavaan 0.6–12. To explore the causal relationship between RAGE229 diet and outcomes

(e.g., homeostatic model of insulin resistance [HOMA-IR]), we fit a path analysis model that includes the direct effect of diet on outcomes and the indirect effect of diet on outcomes via mediators (e.g., adiponectin/fat mass, leptin/fat mass). False discovery rate-adjusted *p* values were reported in multiple hypothesis testing.

The remainder of the detailed descriptions are provided in online Supporting Information Methods.

RESULTS

RAGE229 increases thermogenic capacity, β-adrenergic-stimulated lipolysis, and mitochondrial function in human and mouse adipocytes

To explore the translational implications of findings linking RAGE to obesity, we employed a novel chemical probe that blocks RAGE signaling, RAGE229 [16]. Primary adipocytes derived from the SAT of a healthy human female were differentiated into mature adipocytes (Figure 1A). Treatment with RAGE229 (100 μM) resulted in significantly higher PKA-substrate phosphorylation (Figure 1B,C); higher phosphorylated hormone-sensitive lipase (HSL)/total HSL; and higher phosphorylated p38 mitogen-activated protein kinase (MAPK)/total p38 MAPK versus vehicle (Figure 1D–F). In the presence of the ß-adrenergic stimulus isoproterenol (0.25 μM) (Figure 1G), human adipocytes demonstrated significant increases in glycerol release and PKA-substrate phosphorylation, which was significantly augmented by co-treatment with RAGE229 (Figure 1H–J). Human adipocytes treated with RAGE229 (5 μM) demonstrated significantly higher maximal respiration versus vehicle (Figure 1K,L). No differences were observed in mitochondrial DNA content between RAGE229- and vehicle-treated human adipocytes (Figure 1M).

In parallel studies, mouse C3H10T1/2 cells were differentiated into adipocytes and treated with RAGE229 (Supporting Information Figure S1A). Compared with vehicle, the RAGE229-treated cells (100 μM) demonstrated significantly higher PKA-substrate phosphorylation; phosphorylated HSL-serine 563/total HSL; phosphorylated adipose triglyceride lipase (ATGL)-serine 406/total ATGL; phosphorylated p38 MAPK/total p38 MAPK; and expression of uncoupling protein 1 (UCP1; Supporting Information Figure S1B–H). Co-treatment with the β3-adrenergic agonist CL316,243 (10 μM) and RAGE229 resulted in significantly higher nonesterified fatty acids (NEFA) and glycerol release and PKA-substrate phosphorylation versus CL316,243/vehicle (Supporting Information Figure S1I–M). Differentiated C3H10T1/2 adipocytes treated with RAGE229 (5 μM) displayed significantly higher maximal respiration versus vehicle (Supporting Information Figure S1N,O).

Acute administration of RAGE229–150 ppm diet to adult pair-fed lean male mice decreases body mass and adiposity and increases thermogenesis

To explore the implications of these findings *in vivo*, we administered RAGE229 to lean male C57BL/6J mice and employed a pair-feeding strategy to regulate caloric intake (Figure 2A). Mice were fed 5053 LabDiet (13% kilocalories from fat) to which 150 ppm of RAGE229 was added (RAGE229–150 ppm diet) or the identical 5053 LabDiet to which

RAGE229–150 ppm had not been added (base diet). Mice were pair-fed for 3 days based on administration of an equivalent caloric intake of the “guide group,” which was fed RAGE229–150 ppm diet 1 day in advance of the pair-fed cohorts in order to determine the "next day" caloric intake. After 3 days of pair feeding, lean mice fed RAGE229–150 ppm diet showed significant reduction in body mass (Figure 2B), despite no significant differences in caloric intake versus pair-fed mice fed base diet (Figure 2C).

Rectal temperatures recorded from mice fed RAGE229–150 ppm diet versus base diet-fed mice were significantly higher on days 2 and 3 of pair feeding, suggestive of higher thermogenesis (Figure 2D). The adipose tissue depot masses of eWAT, iWAT, and iBAT were significantly lower in mice pair-fed RAGE229–150 ppm diet versus mice fed caloric equivalents of base diet after 3 days (Figure 2E). Plasma concentrations of NEFA and glycerol (in the fed state) were significantly higher in mice pair-fed RAGE229–150 ppm on day three versus mice pair-fed base diet (Figure 2F,G).

These findings led us to examine the effects of RAGE229 on lipolysis. After 3 days of pair feeding, in iWAT, there were no significant differences in phosphorylated PKA substrates, phosphorylated HSL-serine 563/total HSL, phosphorylated p38/total p38 MAPK, or phosphorylated ATGL-serine 406/total ATGL between RAGE229–150 ppm diet versus base diet pair-fed mice (Figure 2H–M). We examined gene expression in iWAT to assess adipose tissue metabolism, thermogenesis, and inflammation. Significantly lower mRNA expression of cell death-inducing DNA fragmentation factor, alpha subunit-like effector A (Cidea), peroxisome proliferator activated receptor gamma (*Pparg*),and interleukin 6 (*Il6*) was observed in pair-fed RAGE229–150 ppm dietversus base diet-fed mice; there were no diet-dependent differences in mRNA expression of uncoupling protein 1 (*Ucp1*), carnitine palmitoyltransferase 2 (*Cpt2*), PPARG coactivator 1 alpha (*Ppargc1a*), patatin-like phospholipase domain containing 2 (*Pnpla2*), fatty acid synthase (*Fasn*), acyl-coenzyme A (CoA) oxidase 1, palmitoyl (*Acox1*), lipase, hormone sensitive (*Lipe*), carnitine palmitoyltransferase 1a, liver (*Cpt1a*), acyl-CoA dehydrogenase long chain (*Acadl*), monoglyceride lipase (*Mgll*), transcription factor A, mitochondrial (*Tfam*), tumor necrosis factor alpha (*Tnfa*), transforming growth factor, beta induced (*Tgfbi*), chemokine (C- motif) ligand 2 (*Ccl2*), or adhesion G-protein-coupled receptor E1 (*Adgre1*) (Supporting Information Figure S2A,B).

In contrast, eWAT of mice fed RAGE229–150 ppm diet versus base diet after 3 days of pair feeding demonstrated significantly higher phosphorylated PKA substrates, phosphorylated HSL-serine 563/total HSL, and phosphorylated p38/total p38 MAPK (Figure 3A–E). No significant differences were observed in phosphorylated ATGL-serine 406/total ATGL (Figure 3C,F). In eWAT, mRNA expression of *Fasn* was significantly lower in RAGE229–150 ppm versus base diet pair-fed mice and there were no differences in mRNA expression of inflammation-related markers (Supporting Information Figure S3A,B).

In iBAT, after 3 days of pair feeding, phosphorylated HSL-serine 563/total HSL and protein levels of UCP1 were significantly higher in RAGE229–150 ppm diet versus base diet pair-fed mice; no differences were observed in phosphorylated PKA substrates, phosphorylated p38/total p38 MAPK, or phosphorylated ATGL-serine 406/total ATGL (Figure 3G–M). In

iBAT, mRNA expression of Ucp1, Cpt2, Acox1, *Acadl*, and *Tfam* was significantly higher in RAGE229–150 ppm diet versus base diet pair-fed mice (Supporting Information Figure S3C).

Administration of RAGE229–150 ppm diet to adult lean male mice decreases body mass and adiposity and improves metabolic health

We next tested ad libitum feeding to determine the effects of RAGE229. Male mice were fed base diet to age 26 weeks and then randomly assigned to RAGE229–150 ppm diet or base diet (Figure 4A). In contrast to lean mice on base diet that exhibited age-associated gain of body mass of approximately 2.31% ± 2.26% over 6 weeks, lean mice fed RAGE229–150 ppm diet demonstrated an average of 5.6% ± 3.0% loss of body mass (Figure 4B,C). By dual-energy x-ray absorptiometry scanning, mice fed RAGE229–150 ppm diet versus base diet demonstrated significantly lower fat mass, 3.7 ± 0.2 versus 5.2 ± 0.6 g, respectively, without differences in lean mass (Figure 4D). At 10 weeks after diet switch, by indirect calorimetry, energy expenditure (EE) did not differ between the groups (Figure 4E). By ANCOVA (Supporting Information Figure S4A and Table S1), the p value for the effect of RAGE229–150 ppm diet versus base diet on EE was 0.0949. With respect to the difference between RAGE229–150 ppm diet versus base diet on the correlation (slope) between body mass and EE, the p value was 0.0943. There were no significant differences in caloric intake or physical activity, respiratory exchange ratio, VO_2 consumption, and VCO_2 production (Supporting Information Figure S4B–F).

We next assessed whole body metabolic effects of RAGE229. RAGE229–150 ppm diet-fed mice displayed better ability to clear glucose during a glucose tolerance test (GTT), with significantly lower glucose excursions observed at 15 and 30 minutes after intraperitoneal (IP) bolus of glucose (1 g/kg body weight; Figure 4F). When these data were calculated as percentage change to account for differences in fasting concentrations of glucose, there were no significant differences (Supporting Information Figure S4G). In a distinct cohort of mice, significantly lower fasting plasma glucose concentrations were also noted in mice fed RAGE229–150 ppm diet versus base diet (Figure 4G). We tested the effects of RAGE229–150 ppm diet on insulin tolerance; in an insulin tolerance test, significantly lower concentrations of blood glucose were noted at baseline and 30 minutes after IP bolus of insulin (0.85 IU/kg body weight; Figure 4H). When these data were calculated as percentage change to account for fasting concentrations of plasma glucose, there were no differences (Supporting Information Figure S4H). There were no differences in the glucose decay constant between the two groups (Supporting Information Table S2). Fasting concentrations of plasma insulin, HOMA-IR, and glucagon did not differ (Figure 4I,J and Supporting Information Figure S4I, respectively). Plasma concentrations of cholesterol were significantly lower in mice fed RAGE229–150 ppm diet versus base diet (Supporting Information Figure S4J). Although there were no differences in plasma concentrations of triglycerides (Supporting Information Figure S4K), hepatic concentrations of triglycerides were significantly lower in mice fed RAGE229–150 ppm diet versus base diet (Supporting Information Figure S4L). Fasting plasma concentrations of NEFA and glycerol did not differ (Supporting Information Figure S4M,N).

We next measured adipose tissue depot mass at the end of the study. After 12 weeks, significantly lower eWAT mass, but not iWAT or iBAT mass, was noted in mice fed RAGE229–150 ppm diet versus base diet (Figure 4K). There were no significant differences in leptin/fat mass (Figure 4L); however, plasma adiponectin/fat mass and adiponectin/leptin concentration ratio [17–19] were significantly higher in mice fed RAGE229–150 ppm diet versus base diet (Figure 4M,N).

After 6 weeks, in iWAT, mRNA expression of *Cidea*, *Cpt2*, *Pnpla2*, *Fasn*, *Pparg*, *Acox1*, *Lipe*, *Cpt1a*, *Acadl*, *Mgll*, and *Tfam* was significantly higher in mice fed RAGE229–150 ppm diet versus base diet; there were no differences in mRNA expression of *Ucp1* or *Ppargc1a* between the groups (Figure 4O). In eWAT and iBAT, there were no significant differences in mRNA expression of any of these genes (Supporting Information Figure S4O,P). Regarding adipose inflammation, in eWAT and iWAT, there were no significant differences in mRNA expression of *Il6*, *Tnfa*, *Tgfbi*, *Ccl2*, or *Adgre1* (Supporting Information Figure S4Q,R).

Administration of RAGE229–150 ppm diet to adult lean female mice decreases body mass and adiposity and improves metabolic health

To examine potential sex-dependent responses to RAGE229, lean female mice were fed base diet to age 26 weeks and then randomized to RAGE229–150 ppm diet versus base diet (Figure 5A). Female mice switched to RAGE229–150 ppm diet exhibited weight loss over 6 weeks compared with base diet-fed mice (Figure 5B,C). At 8 weeks after diet switch, female mice fed RAGE229–150 ppm diet demonstrated significant reduction in perigonadal white adipose tissue (pWAT) mass, with no significant differences in mass of iWAT or iBAT (Figure 5D). Female mice fed RAGE229–150 ppm diet demonstrated superior ability to clear glucose during a GTT, along with lower fasting concentrations of plasma glucose (Figure 5E,F). When these data were calculated as percentage change to account for fasting concentrations of glucose, there were no significant differences in the area under the curve; however, at 30 minutes, significantly lower glucose concentrations were observed in mice fed RAGE229–150 ppm diet versus base diet (Supporting Information Figure S5A). Significantly lower plasma insulin, HOMA-IR, and cholesterol were noted in female mice fed RAGE229–150 ppm diet versus base diet (Figure 5G,H and Supporting Information Figure S5B, respectively). There were no significant differences in plasma concentrations of triglycerides, NEFA, or glycerol (Supporting Information Figure S5C–E).

We examined gene expression profiles at 8 weeks after diet switch. Comparing mice fed RAGE229–150 ppm diet versus base diet, in iWAT, mRNA expression of *Pnpla2* and *Pparg* was significantly higher (Figure 5I); in pWAT, mRNA expression of Cpt2, *Fasn*, *Pparg*, and *Mgll* was significantly higher (Supporting Information Figure S5F); and in iBAT, expression of *Pparg* was significantly higher and expression of *Acadl* and *Tfam* was significantly lower (Supporting Information Figure S5G). Comparing mice fed RAGE229–150 ppm diet versus base diet, in pWAT, significantly lower mRNA expression of *Ccl2* and *Adgre1* was observed; and in iWAT, significantly lower expression of *Tgfbi* and *Adgre1* was noted (Supporting Information Figure S5H,I).

Administration of RAGE229–150 ppm diet to pair-fed male mice with established obesity undergoing dietinduced weight loss increases thermogenesis

Next, we asked whether RAGE229 affected body mass and thermogenesis in mice with established HFD-induced obesity undergoing dietinduced weight loss. We pair-fed mice to regulate caloric intake and monitored rectal temperature after switching from HFD (60% kilocalories from fat) to RAGE229–150 ppm diet versus base diet (Figure 6A). Upon switch from HFD to diets lower in fat, reductions in body temperature have been demonstrated [20, 21]. Mice switched to RAGE229–150 ppm diet showed significantly less decline in body temperature versus base diet-fed mice (Figure 6B). Significant differences in change in rectal temperature were seen on days 2 to 5, 8 to 11, and 16, and the overall loss of body temperature was less in RAGE229–150 ppm diet group (Figure 6B). Over this period, the percentage loss of body mass was higher in RAGE229–150 ppm diet group versus base diet group, which reached statistical significance after day 24, after which RAGE229–150 ppm diet-fed mice still showed further decline in body mass in comparison to base diet-fed mice (Figure 6C). Thus, RAGE229–150 ppm diet contributed to regulation of heat dissipation in mice with obesity undergoing diet-induced weight loss.

Administration of RAGE229–150 ppm diet to male mice with established obesity undergoing diet-induced weight loss accelerates loss of body mass and adiposity and metabolic recovery

To probe for the effects of RAGE229–150 ppm diet in mice with obesity, male mice were fed HFD for 18 weeks (ad libitum) and then assigned into two weight-matched groups, which were then randomly assigned to RAGE229–150 ppm diet or to base diet (13% kiloalories from fat) (Figure 7A). Mice with obesity switched to RAGE229–150 ppm diet lost significantly more body mass than mice switched to base diet over 6 weeks (Figure 7B). Mice fed RAGE229–150 ppm diet lost 33% of their initial body mass whereas mice fed base diet lost 19% of their initial body mass (Figure 7C). At 9 weeks after diet switch, by dual-energy x-ray absorptiometry, mice with obesity fed RAGE229–150 ppm diet versus base diet exhibited no significant differences in lean mass; however, fat mass was significantly lower, 4.6 ± 0.6 g versus 6.6 ± 1.2 g, respectively (Figure 7D). At 10 weeks after diet switch, there were no differences in EE (Figure 7E). By ANCOVA, the p value for the effect of RAGE229–150 ppm diet versus base diet on EE was 0.1356, and, with respect to the difference between RAGE229–150 ppm diet versus base diet on the correlation (slope) between body mass and EE, the p value was 0.1294 (Supporting Information Table S3 and Figure S6A). There were no significant differences in caloric intake or physical activity, respiratory exchange ratio, VO_2 consumption, and VCO_2 production between the groups (Supporting Information Figure S6B–F).

In mice with established obesity and switched to RAGE229–150 ppm diet versus base diet after 6 weeks, superior clearance of glucose was noted (Figure 7F); fasting concentrations of blood glucose were not different (Figure 7G). Mice fed RAGE229–150 ppm diet versus base diet displayed significantly better insulin tolerance (Supporting Information Figure S6G). When these data were calculated as percentage change to account for fasting concentrations of glucose, there were no significant differences between groups (Supporting Information

Figure S6H). Furthermore, there were no differences in the glucose decay constant between the groups (Supporting Information Table S4).

To further probe the potential effects of RAGE229–150 ppm diet on insulin sensitivity, we performed an *in vivo* insulin signaling study; after a 6-hour fast, insulin was administered by IP injection, followed by sacrifice of mice at 15 minutes after injection. First, we examined concentrations of glucose before insulin injection, followed by the 15-minute time point after injection. As indicated in Supporting Information Figure S6I, although there were no significant differences in plasma concentrations of glucose before and 15 minutes after insulin injection in base diet-fed mice, mice fed RAGE229–150 ppm diet displayed significantly lower plasma concentrations of glucose after and before injection of insulin. Furthermore, plasma concentrations of glucose were significantly lower in RAGE229–150 ppm diet-fed mice versus base diet-fed mice, both at the pre-insulin injection time point and at the 15-minute post-insulin injection time point (Supporting Information Figure S6I). As shown in the inset to Supporting Information Figure S6I, the percentage reduction in plasma concentrations of glucose over the time course (before insulin to 15 minutes after insulin injection) was significantly greater in mice fed RAGE229–150 ppm diet versus base diet.

Second, consistent with these observations, Western blotting experiments revealed significantly higher phosphorylation of AKT-serine473/total AKT in both liver and muscle tissues of mice fed RAGE229–150 ppm diet versus base diet at 15 minutes after insulin injection (Figure 7H,I). In contrast, no differences were observed in eWAT and iWAT (Supporting Information Figure S6J,K). Furthermore, phosphorylated insulin receptor β-tyrosine 1150/1151/total insulin receptor β was significantly higher in liver tissue of mice fed RAGE229–150 ppm diet versus base diet; no differences were observed in muscle, eWAT, or iWAT of these mice (Supporting Information Figure S6L,M). In addition to these findings suggesting improved insulin sensitivity in mice fed RAGE229–150 ppm diet, fasting plasma concentrations of insulin and HOMA-IR were significantly lower in mice fed RAGE229–150 ppm diet versus base diet (Figure 7J,K).

No differences were observed in concentrations of plasma glucagon (Supporting Information Figure S6N). Plasma cholesterol concentrations were significantly lower between groups (Supporting Information Figure S6O). Although plasma triglyceride concentrations did not differ, hepatic triglyceride concentrations were significantly lower in mice fed RAGE229–150 ppm diet versus base diet (Supporting Information Figure S6P,Q). At 12 weeks after diet switch, there were no significant differences in fasting plasma concentrations of NEFA or glycerol (Supporting Information Figure S6R,S). However, at 12 weeks after diet switch, in a distinct cohort of mice subjected to the conditions in Figure 7A, but sacrificed in the fed state, plasma concentrations of NEFA, but not glycerol, were significantly higher in mice fed RAGE229–150 ppm diet versus base diet (Figure 7L,M).

At 12 weeks after diet switch, mice fed RAGE229–150 ppm diet demonstrated significantly lower mass of eWAT and iWAT, but not iBAT, compared with base diet-fed mice (Figure 7N). Compared with mice fed base diet after HFD, mice fed RAGE229–150 ppm diet demonstrated significantly lower leptin/fat mass and significantly higher adiponectin/fat mass and adiponectin/leptin concentration ratio (Figure 7O–Q). As these findings suggested

differences in adipose tissue remodeling, we measured adipocyte size. In eWAT, adipocyte area was significantly lower in mice fed RAGE229–150 ppm diet versus base diet 12 weeks after diet switch (Supporting Information Figure S6T). Comparison of eWAT adipocyte area distribution (percentage) of mice fed RAGE229–150 ppm diet versus base diet showed a significantly higher number of smaller adipocytes and a lower number of larger adipocytes (Supporting Information Figure S6U). In iWAT, no differences were observed in adipocyte area between the groups (Supporting Information Figure S6V,W).

On account of the effects of RAGE229–150 ppm diet versus base diet on insulin sensitivity measures in mice with obesity undergoing weight loss after HFD feeding, as demonstrated by the *in vivo* insulin signaling study, fasting concentrations of insulin, and HOMA-IR, to begin to identify potential mechanisms by which interruption of RAGE signaling exerted these effects, we performed mediation analyses. As illustrated in Supporting Information Table S5 and Figure S6X–Z, we employed HOMA-IR as "Y" to reflect a measure of insulin sensitivity and tested multiple potential mediating factors ("X"), that is, factors through which RAGE229–150 ppm diet might have exerted its beneficial effects on HOMA-IR, including the following: weight loss, fat mass, leptin/fat mass, adiponectin/fat mass, adiponectin/leptin concentration ratio, plasma concentrations of cholesterol, and hepatic triglyceride content.

After correction for multiple comparisons (false discovery rate), the indirect effect, that is the mediation effect, was significant only for the (X) putative mediators of fat mass, leptin/fat mass, adiponectin/fat mass, and adiponectin/leptin concentration ratio. The coefficient "Group X Y" in Supporting Information Table S5 indicates the effect of RAGE229–150 ppm diet on HOMA-IR through X. In order to support conclusions regarding mediation of RAGE229–150 ppm diet through X on Y, Group X Y must be a negative value. Therefore, in this analysis, Group X Y is a negative value in the cases of leptin/fat mass, adiponectin/fat mass, and adiponectin/leptin ratio. These data suggest that these three factors, leptin/fat mass, adiponectin/fat mass, and adiponectin/leptin ratio, may contribute to mediating the effects of RAGE229–150 ppm diet on the lower HOMA-IR index.

Next, we assessed the effects of RAGE229 on activation of PKA and its targets in mice fed HFD and then switched to either RAGE229–150 ppm or base diet. Mice were euthanized in the fed state at 6 weeks after diet switch. In iWAT of mice fed RAGE229–150 ppm diet versus base diet, significantly higher PKA-substrate phosphorylation, phosphorylated of HSL-serine 563/total HSL, and phosphorylated p38/total p38 MAPK were observed (Figure 8A–F); no differences were observed in phosphorylated ATGL-serine 406/total ATGL (Figure 8C,E). In eWAT and iBAT, there were no significant differences in phosphorylated PKA substrates, phosphorylated HSL-serine 563/total HSL, phosphorylated p38/total p38 MAPK, or phosphorylated ATGL/total ATGL; in iBAT, there were no significant differences in UCP1 protein (Supporting Information Figure S7A–F and H–N).

We next examined gene expression at 6 weeks after diet switch. Comparing mice fed RAGE229–150 ppm diet versus base diet, in iWAT, mRNA expression of *Ppargc1a* and *Mgll* was significantly higher (Figure 8G); in eWAT and iBAT, there were no differences in mRNA expression of any of the genes noted earlier (Supporting Information Figure S7G,O).

There were no significant differences in UCP1 protein (immunostaining) at 12 weeks after diet switch in iWAT and iBAT (Supporting Information Figure S7P,Q).

To probe for potential effects of RAGE229–150 ppm diet on adipose tissue inflammation, we examined crown-like structures (CLS). In mice with HFD-induced obesity, at 12 weeks after switching to RAGE229–150 ppm diet versus base diet, there were no significant differences in eWAT CLS by quantification of F4/80 (macrophage) epitopes (Supporting Information Figure S7R). At 6 weeks after diet switch, comparing mice fed RAGE229–150 ppm diet versus base diet, in eWAT, mRNA expression of *Tnfα* was significantly lower (Supporting Information Figure S7S); in iWAT, there were no significant differences in CLS or mRNA expression of any of the genes linked to inflammation (Supporting Information Figure S7T,U).

Effects of RAGE229 diet in lean mice and in mice with obesity are dose dependent

In previous work, we observed dose-dependent effects of RAGE229 in mice with types 1 or 2 diabetes [16]. Therefore, here, we tested threefold less RAGE229 ("RAGE229–50 ppm diet"). When lean male mice were switched to RAGE229–50 ppm diet versus base diet (Supporting Information Figure S8A), there were no significant differences in body mass or mass of eWAT, iWAT, or iBAT (Supporting Information Figure S8B,C). There were no differences in the GTT or in concentrations of fasting plasma glucose or insulin or HOMA-IR (Supporting Information Figure S8D–G). Plasma concentrations of cholesterol, triglycerides, NEFA, or glycerol did not differ (Supporting Information Figure S8H–K).

In a distinct study, male mice were fed HFD for 18 weeks to establish obesity and were then switched to RAGE229–50 ppm diet or base diet (Supporting Information Figure S9A). Both groups of mice lost body mass; however, there were no significant differences between the diets (Supporting Information Figure S9B). Twelve weeks after HFD switch, there were no significant differences in eWAT, iWAT, or iBAT mass by diet (Supporting Information Figure S9C). In the GTT, at the 15-minute time point, significantly lower concentrations of plasma glucose were observed in mice fed RAGE229–50 ppm diet versus base diet (Supporting Information Figure S9D); fasting plasma glucose concentrations were also significantly lower (Supporting Information Figure S9E). There were no significant differences in plasma concentrations of insulin, HOMA-IR, or plasma concentrations of triglycerides, NEFA, or glycerol (Supporting Information Figure S9F–K). Plasma concentrations of cholesterol were significantly lower in mice fed RAGE229–50 ppm diet versus base diet (Supporting Information Figure S9H).

DISCUSSION

In this study, we demonstrate that pharmacological antagonism of RAGE by the chemical probe RAGE229 promoted reductions in body mass and adiposity and improvements in whole body metabolism in male or female lean mice and in male mice with obesity undergoing weight loss, in a manner independent of caloric intake, as demonstrated through testing via pair-feeding methodologies or through measurements in metabolic chambers. RAGE229 also had no effect on physical activity. Rather, the benefits of RAGE229 were traced, at least in part, to cell-intrinsic roles in adipocytes, as RAGE229

enhanced phosphorylation of PKA targets, including mediators of lipolysis, and augmented phosphorylation of p38 MAPK, which plays key roles in PKA-driven thermogenic programs in adipocytes [22, 23].

Here, we restricted the investigation of mice with obesity undergoing weight loss to male mice, as female mice are relatively protected from HFD-induced obesity [24–27]. Although RAGE229 exerted similar benefits in lean male and female mice with respect to body mass and composition, interesting adipose depot-dependent differences were observed. In lean male mice, RAGE229 exerted its greatest effects in iWAT, with upregulation of multiple genes linked to lipolysis, fatty acid oxidation, and mitochondrial biogenesis. In lean female mice fed RAGE229, the effects were noted in pWAT, iWAT, and iBAT. These data are consistent with previous reports indicating sex differences in pWAT versus iWAT in human and rodent females versus males, in whom sex hormones and innate differences in adipocytes, adipocyte precursors, and immune cells may contribute [27–30].

In parallel with RAGE229-mediated loss of body mass and adiposity, insulin and/or glucose metabolism was improved by this treatment. Feeding the RAGE229–150 ppm diet beneficially affected multiple pathways associated with improvements in glucose and insulin sensitivity, including reductions in hepatic triglycerides [31] and increased plasma concentrations of adiponectin and adiponectin/leptin concentration ratio [32–34], and, in the obese mice undergoing weight loss, RAGE229 resulted in reduced adipocyte area [35]. Interestingly, the eWAT and/or iWAT depots of the mice under study treated with RAGE229 revealed only modest differences in mRNA expression of cytokines and chemokines. Thus, we surmise that the primary effects of RAGE229 on insulin tolerance are not likely to be predominantly driven by inflammation.

We acknowledge study limitations. First, pair-feeding administration of RAGE229 to lean mice or to mice with obesity undergoing weight loss resulted in higher rectal temperatures and enhanced adipose tissue thermogenic programs in a manner independent of caloric intake compared with mice fed base diet. However, EE did not significantly differ between diet groups. It is notable that there are precedents for these seemingly discordant findings, even in human studies. Specifically, when the β3-adrenergic receptor agonist mirabegron was administered to lean male humans, an increase in armpit temperature, used as a surrogate for core body temperature [36], was observed [37]. In parallel, the humans treated with mirabegron demonstrated an increase in serum free fatty acids, yet no differences in EE were observed, as assessed by indirect calorimetry [37]. These considerations illustrate that our future studies should include the use of more sensitive techniques to measure EE, such as doubly labeled water [38].

Second, it is acknowledged that the novel chemical probe RAGE229 is a key first step toward eventual clinical trial testing in humans. In human SAT-derived adipocytes and in mice and mouse C3H10T1/2 differentiated adipocytes, RAGE229 augmented lipolysis. We propose that these results accounted, at least in part, for the reduced triglyceride content observed in the mouse liver. This finding buttresses earlier studies that reported lipolysis in early stages of weight loss in mice [39]. In female humans, lipolysis was increased during successful rapid weight loss [40]. Furthermore, it was shown that ß3-

adrenergic receptors are essential in human brown and beige adipocytes for the regulation of lipolysis and thermogenesis [41]. Although increased products of lipolysis may be associated with insulin resistance and hepatic steatosis [42], in the RAGE229–150 ppm diet-metabolic milieu, we surmise that the overall improvements in metabolism are accounted for by the complementary and integrated benefits of the RAGE229–150 ppm diet in the liver and adipocytes (concentrations of hepatic triglycerides and plasma concentration of adiponectin and leptin). Published work supports this contention, as lipolysis-associated insulin resistance may be related to the acute versus the chronic nature of the stress [43]. Collectively, these considerations suggest that, although not yet tested in humans, the overall metabolic benefits of RAGE229 may outweigh any consequences of increased lipolysis, at least based on these studies in a murine model.

In summary, we conclude that targeting the RAGE signaling pathway may re-equilibrate thermogenic programs and thereby promote healthful body mass and composition and metabolic fitness.

Supplementary Material

Refer to Web version on PubMed Central for supplementary material.

ACKNOWLEDGMENTS

The authors gratefully acknowledge the expert assistance of Latoya Woods of the Diabetes Research Program, Department of Medicine, New York University Grossman School of Medicine, in the preparation of this manuscript.

FUNDING INFORMATION

American Heart Association Strategically Focused Network on Obesity 17SFRN33490004 (Ann Marie Schmidt); US Public Health Service: 1P01HL131481 (Ann Marie Schmidt and Ravichandran Ramasamy), 1P01HL146367 (Ann Marie Schmidt, Ravichandran Ramasamy, Alexander Shekhtman), 1R01DK122456 (Ann Marie Schmidt, Ravichandran Ramasamy, Alexander Shekhtman) and 5K01DK120782-02 (Henry H. Ruiz); and the NYU Histology Core, which is partially supported by New York University Cancer Institute Cancer Center Support Grant 5P30CA016087-31. Support was also provided from the Diabetes Research Program, New York University Grossman School of Medicine.

DATA AVAILABILITY STATEMENT

After publication, all reasonable requests will be fulfilled. Any materials reported in this research are available through Material Transfer Agreement with New York University Grossman School of Medicine.

REFERENCES

1. Ruiz HH, Ramasamy R, Schmidt AM. Advanced glycation end products: building on the concept of the "common soil" in metabolic disease. Endocrinology. 2020;161:bqz006. doi:10.1210/endocr/bqz006 [PubMed: 31638645]
2. Kremers SHM, Remmelzwaal S, Schalkwijk CG, et al. The role of serum and dietary advanced glycation endproducts in relation to cardiac function and structure: the Hoorn Study. Nutr Metab Cardiovasc Dis. 2021;31:3167–3175. [PubMed: 34518083]

3. Gaens KH, Stehouwer CD, Schalkwijk CG. The N(ε)-(carboxymethyl) lysine-RAGE axis: putative implications for the pathogenesis of obesity-related complications. Expert Rev Endocrinol Metab. 2010;5:839–854. [PubMed: 30780826]
4. Uribarri J, Cai W, Ramdas M, et al. Restriction of advanced glycation end products improves insulin resistance in human type 2 diabetes: potential role of AGER1 and SIRT1. Diabetes Care. 2011;34:1610–1616. [PubMed: 21709297]
5. Egaña-Gorroño L, López-Díez R, Yepuri G, et al. Receptor for advanced glycation end products (RAGE) and mechanisms and therapeutic opportunities in diabetes and cardiovascular disease: insights from human subjects and animal models. Front Cardiovasc Med. 2020;7:37. doi:10.3389/fcvm.2020.00037 [PubMed: 32211423]
6. Gaens KH, Goossens GH, Niessen PM, et al. Nε-(carboxymethyl) lysine-receptor for advanced glycation end product axis is a key modulator of obesity-induced dysregulation of adipokine expression and insulin resistance. Arterioscler Thromb Vasc Biol. 2014;34:1199–1208. [PubMed: 24723555]
7. Song F, Hurtado del Pozo C, Rosario R, et al. RAGE regulates the metabolic and inflammatory response to high-fat feeding in mice. Diabetes. 2014;63:1948–1965. [PubMed: 24520121]
8. Monden M, Koyama H, Otsuka Y, et al. Receptor for advanced glycation end products regulates adipocyte hypertrophy and insulin sensitivity in mice: involvement of Toll-like receptor 2. Diabetes. 2013;62:478–489. [PubMed: 23011593]
9. Feng Z, Du Z, Shu X, et al. Role of RAGE in obesity-induced adipose tissue inflammation and insulin resistance. Cell Death Discov. 2021;7:305. doi:10.1038/s41420-021-00711-w [PubMed: 34686659]
10. Hurtado Del Pozo C, Ruiz HH, Arivazhagan L, et al. A receptor of the immunoglobulin superfamily regulates adaptive thermogenesis. Cell Rep. 2019;28:773–791.e777. [PubMed: 31315054]
11. Kim HJ, Jeong MS, Jang SB. Molecular characteristics of RAGE and advances in small-molecule inhibitors. Int J Mol Sci. 2021;22:6904. doi:10.3390/ijms22136904 [PubMed: 34199060]
12. Bongarzone S, Savickas V, Luzi F, Gee AD. Targeting the receptor for advanced glycation endproducts (RAGE): a medicinal chemistry perspective. J Med Chem. 2017;60:7213–7232. [PubMed: 28482155]
13. Hudson BI, Kalea AZ, Del Mar AM, et al. Interaction of the RAGE cytoplasmic domain with diaphanous-1 is required for ligand-stimulated cellular migration through activation of Rac1 and Cdc42. J Biol Chem. 2008;283:34457–34468. [PubMed: 18922799]
14. Rai V, Maldonado AY, Burz DS, et al. Signal transduction in receptor for advanced glycation end products (RAGE): solution structure of Cterminal rage (ctRAGE) and its binding to mDia1. J Biol Chem. 2012;287:5133–5144. [PubMed: 22194616]
15. Manigrasso MB, Pan J, Rai V, et al. Small molecule inhibition of ligand-stimulated RAGE-DIAPH1 signal transduction. Sci Rep. 2016;6:22450. doi:10.1038/srep22450 [PubMed: 26936329]
16. Manigrasso MB, Rabbani P, Egaña-Gorroño L, et al. Small-molecule antagonism of the interaction of the RAGE cytoplasmic domain with DIAPH1 reduces diabetic complications in mice. Sci Transl Med. 2021;13:eabf7084. doi:10.1126/scitranslmed.abf7084 [PubMed: 34818060]
17. Frühbeck G, Catalán V, Rodríguez A, et al. Involvement of the leptin-adiponectin axis in inflammation and oxidative stress in the metabolic syndrome. Sci Rep. 2017;7:6619. doi:10.1038/s41598-017-06997-0 [PubMed: 28747790]
18. Unamuno X, Izaguirre M, Gomez-Ambrosi J, et al. Increase of the adiponectin/leptin ratio in patients with obesity and type 2 diabetes after Roux-en-Y gastric bypass. Nutrients. 2019;11:2069. doi:10.3390/nu11092069 [PubMed: 31484347]
19. Becerril S, Rodríguez A, Catalán V, et al. Sex- and age-dependent changes in the adiponectin/leptin ratio in experimental diet-induced obesity in mice. Nutrients. 2022;15:73. doi:10.3390/nu15010073 [PubMed: 36615734]
20. Carrillo AE, Flouris AD. Caloric restriction and longevity: effects of reduced body temperature. Ageing Res Rev. 2011;10:153–162. [PubMed: 20969980]
21. Guijas C, Montenegro-Burke JR, Cintron-Colon R, et al. Metabolic adaptation to calorie restriction. Sci Signal. 2020;13:eabb2490. doi:10.1126/scisignal.abb2490 [PubMed: 32900879]

22. Robidoux J, Cao W, Quan H, et al. Selective activation of mitogenactivated protein (MAP) kinase kinase 3 and p38alpha MAP kinase is essential for cyclic AMP-dependent UCP1 expression in adipocytes. Mol Cell Biol. 2005;25:5466–5479. [PubMed: 15964803]
23. Cao W, Daniel KW, Robidoux J, et al. p38 mitogen-activated protein kinase is the central regulator of cyclic AMP-dependent transcription of the brown fat uncoupling protein 1 gene. Mol Cell Biol. 2004;24:3057–3067. [PubMed: 15024092]
24. Hwang LL, Wang CH, Li TL, et al. Sex differences in high-fat dietinduced obesity, metabolic alterations and learning, and synaptic plasticity deficits in mice. Obesity (Silver Spring). 2010;18:463–469. [PubMed: 19730425]
25. Pettersson US, Waldén TB, Carlsson PO, Jansson L, Phillipson M. Female mice are protected against high-fat diet induced metabolic syndrome and increase the regulatory T cell population in adipose tissue. PLoS One. 2012;7:e46057. doi:10.1371/journal.pone.0046057 [PubMed: 23049932]
26. Casimiro I, Stull ND, Tersey SA, Mirmira RG. Phenotypic sexual dimorphism in response to dietary fat manipulation in C57BL/6J mice. J Diabetes Complications. 2021;35:107795. doi:10.1016/j.jdiacomp.2020.107795 [PubMed: 33308894]
27. Singer K, Maley N, Mergian T, et al. Differences in hematopoietic stem cells contribute to sexually dimorphic inflammatory responses to high fat diet-induced obesity. J Biol Chem. 2015;290:13250–13262. [PubMed: 25869128]
28. Shan B, Barker CS, Shao M, Zhang Q, Gupta RK, Wu Y. Multilayered omics reveal sex- and depot-dependent adipose progenitor cell heterogeneity. Cell Metab. 2022;34:783–799.e787. [PubMed: 35447091]
29. Maric I, Krieger J-P, van der Velden P, et al. Sex and species differences in the development of diet-induced obesity and metabolic disturbances in rodents. Front Nutr. 2022;9:2022.828522. doi:10.3389/fnut.2022.828522
30. Lee M-J, Fried SK. Sex-dependent depot differences in adipose tissue development and function; role of sex steroids. J Obes Metab Syndr. 2017;26:172–180. [PubMed: 31089514]
31. Mayerson AB, Hundal RS, Dufour S, et al. The effects of rosiglitazone on insulin sensitivity, lipolysis, and hepatic and skeletal muscle triglyceride content in patients with type 2 diabetes. Diabetes. 2002;51:797–802. [PubMed: 11872682]
32. Havel PJ. Control of energy homeostasis and insulin action by adipocyte hormones: leptin, acylation stimulating protein, and adiponectin. Curr Opin Lipidol. 2002;13:51–59. [PubMed: 11790963]
33. Koh EH, Park JY, Park HS, et al. Essential role of mitochondrial function in adiponectin synthesis in adipocytes. Diabetes. 2007;56:2973–2981. [PubMed: 17827403]
34. Li X, Zhang D, Vatner DF, et al. Mechanisms by which adiponectin reverses high fat diet-induced insulin resistance in mice. Proc Natl Acad Sci U S A. 2020;117:32584–32593. [PubMed: 33293421]
35. Puri V, Ranjit S, Konda S, et al. Cidea is associated with lipid droplets and insulin sensitivity in humans. Proc Natl Acad Sci U S A. 2008;105:7833–7838. [PubMed: 18509062]
36. Lodha R, Mukerji N, Sinha N, Pandey RM, Jain Y. Is axillary temperature an appropriate surrogate for core temperature? Indian J Pediatr. 2000;67:571–574. [PubMed: 10984997]
37. Nahon KJ, Janssen LGM, Sardjoe Mishre ASD, et al. The effect of mirabegron on energy expenditure and brown adipose tissue in healthy lean South Asian and Europid men. Diabetes Obes Metab. 2020;22:2032–2044. [PubMed: 32558052]
38. Coward WA. Stable isotopic methods for measuring energy expenditure. The doubly-labelled-water (2H2(18)O) method: principles and practice. Proc Nutr Soc. 1988;47:209–218. [PubMed: 3076004]
39. Kosteli A, Sugaru E, Haemmerle G, et al. Weight loss and lipolysis promote a dynamic immune response in murine adipose tissue. J Clin Invest. 2010;120:3466–3479. [PubMed: 20877011]
40. Alemán JO, Iyengar NM, Walker JM, et al. Effects of rapid weight loss on systemic and adipose tissue inflammation and metabolism in obese postmenopausal women. J Endocr Soc. 2017;1:625–637. [PubMed: 29264516]

41. Cero C, Lea HJ, Zhu KY, Shamsi F, Tseng YH, Cypess AM. β3-Adrenergic receptors regulate human brown/beige adipocyte lipolysis and thermogenesis. JCI Insight. 2021;6:e139160. doi:10.1172/jci.insight.139160 [PubMed: 34100382]

42. Morigny P, Houssier M, Mouisel E, Langin D. Adipocyte lipolysis and insulin resistance. Biochimie. 2016;125:259–266. [PubMed: 26542285]

43. Raje V, Ahern KW, Martinez BA, et al. Adipocyte lipolysis drives acute stress-induced insulin resistance. Sci Rep. 2020;10:18166. doi:10.1038/s41598-020-75321-0 [PubMed: 33097799]

Study Importance

What is already known?

- In mice, global or adipocyte-specific deletion of *Ager* (the gene encoding receptor for advanced glycation end products [RAGE]) protects mice from diet-induced obesity through upregulation of thermogenic programs. We recently discovered a novel chemical probe, called RAGE229, that blocks RAGE signal transduction and assuages inflammation and diabetic complications in mice. Here, we tested whether RAGE229 modulates body mass and composition and metabolism in mice.

What does this study add?

- We demonstrate that male or female lean adult mice or male mice with obesity undergoing weight loss and fed RAGE229-diet versus the base diet display superior reductions in body mass and adiposity and improvements in glucose, insulin, and lipid metabolism in a manner independent of caloric intake or physical activity. The mediating mechanisms were traced to upregulation of protein kinase A-mediated stimulation of lipolysis, mitochondrial function, and thermogenesis in adipose tissue and in human and mouse adipocytes.

How might these results change the direction of research or the focus of clinical practice?

- These findings suggest that future studies employing treatment with RAGE signaling inhibitors in chronic inflammatory states or diabetes may have added benefit of stimulating healthful body composition and metabolism.

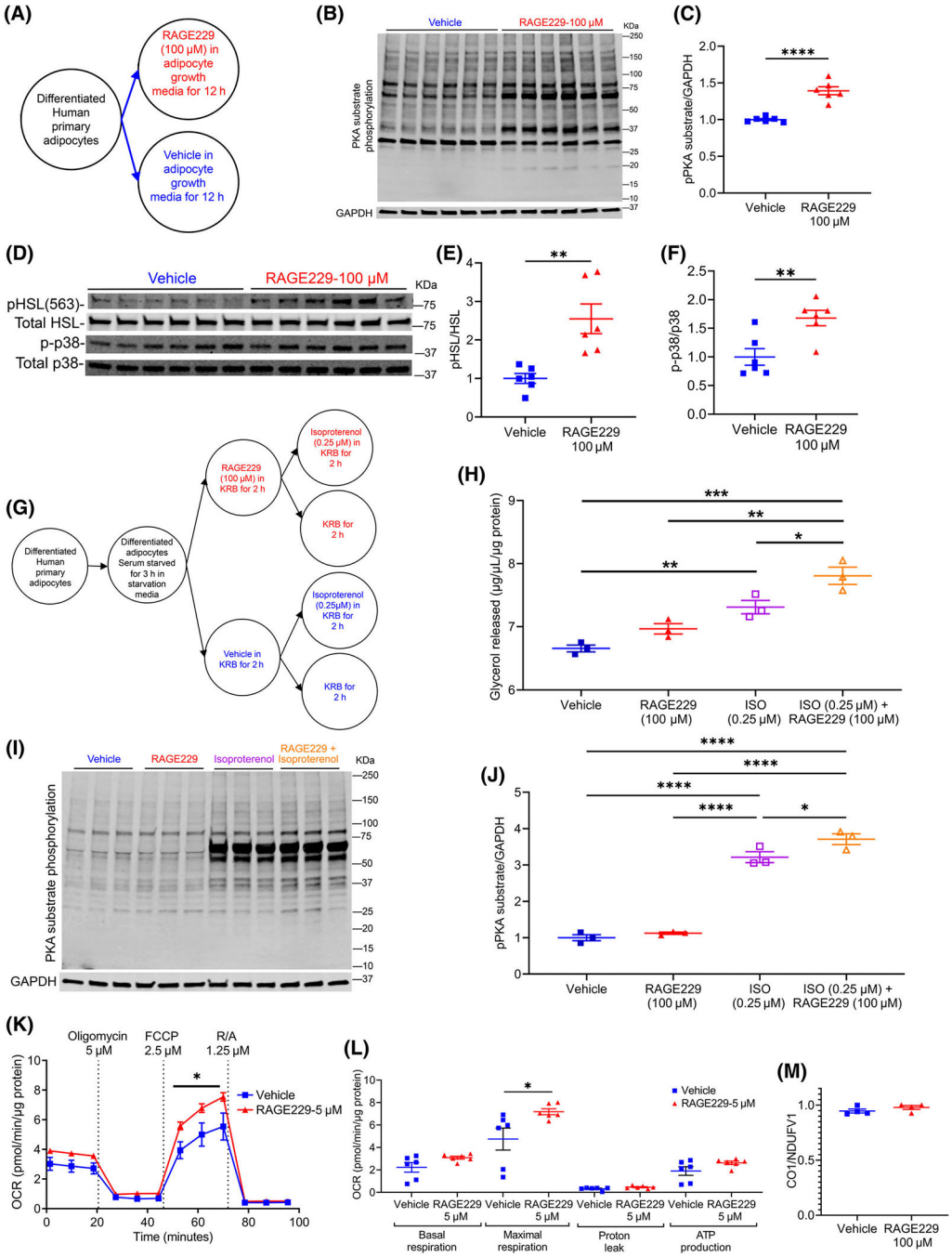

FIGURE 1.

Treatment of human adipocytes with RAGE229 increases PKA-substrate phosphorylation, β-adrenergic-stimulated lipolysis, and mitochondrial function. (A) Experimental schematic: differentiated human subcutaneous adipose tissue-derived adipocytes treated with RAGE229 (100 μM) or vehicle (DMSO) in growth media for 12 hours (n = 6 independent wells of the tissue culture plate per treatment group; data presented from one of the two independent experiments; each independent experiment contained a total of n = 6 independent replicates per treatment group). (B–F) Western blot analysis of cell lysate probed for expression

of PKA-substrate phosphorylation/glyceraldehyde-3-phosphate dehydrogenase (GAPDH), phosphorylated HSL-serine 563/total HSL, and phosphorylated p38/total p38 MAPK. (G) Experimental schematic: differentiated human adipocytes as in panel A were serum-starved for 3 hours before treatment with either RAGE229 (100 μM) or vehicle (DMSO) for 2 hours followed by isoproterenol (ISO; 0.25 μM) treatment for 2 hours ($n = 3$ independent wells of the tissue culture plate per treatment group; data presented from one of the two independent experiments; each independent experiment contained a total of $n = 3$ independent replicates per treatment group). (H) Glycerol released into KRB after ISO treatment. (I–J) Western blot analysis of cell lysate for expression of PKA-substrate phosphorylation/GAPDH. (K,L) OCR measured in adipocytes pretreated with vehicle vs. RAGE229 (5 μM) for 2 hours ($n = 6$ independent wells of the plate per treatment group; data presented from one of the two independent experiments; each independent experiment contained a total of $n = 6$ independent replicates per treatment group). (M) Mitochondrial DNA content presented as the ratio of CO1/NDUFV1 in adipocytes pretreated with vehicle vs. RAGE229 (5 μM) for 2 hours ($n = 4$ independent experimental wells of the tissue culture plate per treatment group). Data are presented as the mean ± SEM. For group comparison, the Shapiro–Wilk normality test was conducted first for each group with prespecified significance level of 0.1, and if passed, the *t* test was implemented whereas the nonparametric Wilcoxon rank sum test was used if normality was not established. Linear mixed-effect model was adopted for correlated/time-series data with post hoc *t* test for group comparisons at each time point. For panels H and J, two-way ANOVA followed by multiple comparison without correction was used to compare groups. KRB, Kreb's Ringer Bicarbonate buffer; OCR, oxygen consumption rate; RAGE229, receptor for advanced glycation end products; R/A, rotenone / antimycin A; CO1, cytochrome C oxidase subunit 1; NDUFV1, NADH:ubiquinone oxidoreductase core subunit V1. *$p < 0.05$; **$p < 0.01$; ***$p < 0.001$; ****$p < 0.0001$ [Color figure can be viewed at wileyonlinelibrary.com]

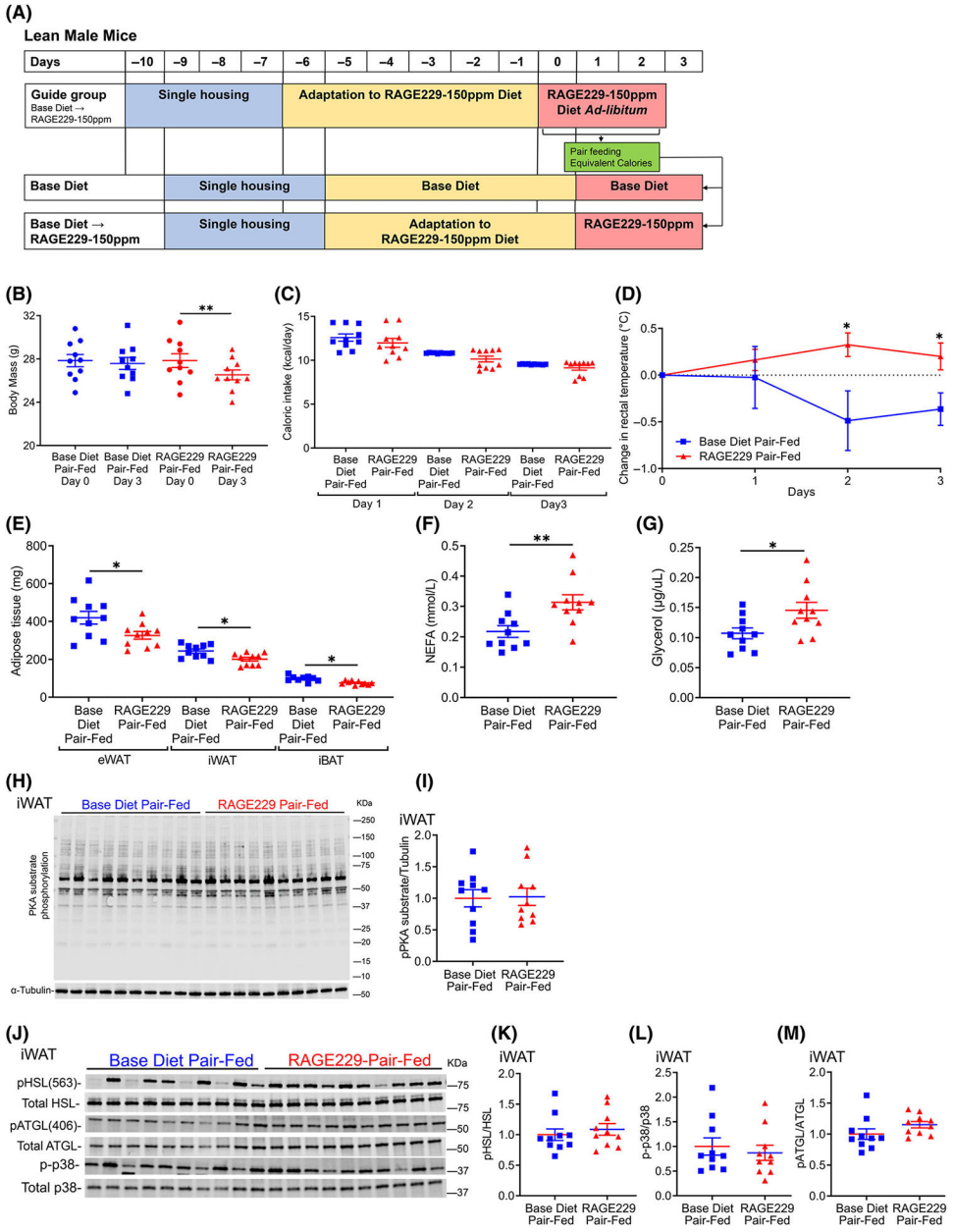

FIGURE 2.

Pair feeding of lean male mice with RAGE229–150 ppm diet reduces body mass and results in higher rectal temperature and plasma concentrations of NEFA and glycerol compared with mice fed base diet. (A) Experimental schematic. (B) Body mass on day 0 and day 3 of pair feeding equivalent calories of either RAGE229–150 ppm or base diet (n = 10 per group). (C) Caloric intake over 3 days of pair feeding. (D) Daily rectal temperature measurements in pair-fed mice after diet switch (n = 8 per group). (E) Adipose tissue depot mass collected after 3 days of pair feeding (n = 9–10 base diet, n = 10 RAGE229–150 ppm diet). (F,G) Randomly fed plasma NEFA and glycerol after 3 days of pair feeding (n = 10 per group). (H–M) Western blot analysis of iWAT lysate collected from randomly fed mice after 3 days of pair feeding probed for expression of PKA-substrate phosphorylation/α-

tubulin, phosphorylated HSL-serine 563/total HSL, phosphorylated p38/total p38 MAPK, and phosphorylated ATGL-serine 406/total ATGL ($n = 10$ per group). Data are presented as the mean ± SEM. Linear mixed-effect model was adopted for correlated/time-series data (panel D) with post hoc t test for group comparisons at each time point. For group comparison, the Shapiro–Wilk normality test was conducted first for each group with prespecified significance level of 0.1, and if passed, the t test was implemented, whereas the nonparametric Wilcoxon rank sum test was used if normality was not established. iWAT, inguinal white adipose tissue; RAGE229, receptor for advanced glycation end products. *$p < 0.05$; **$p < 0.01$ [Color figure can be viewed at wileyonlinelibrary.com]

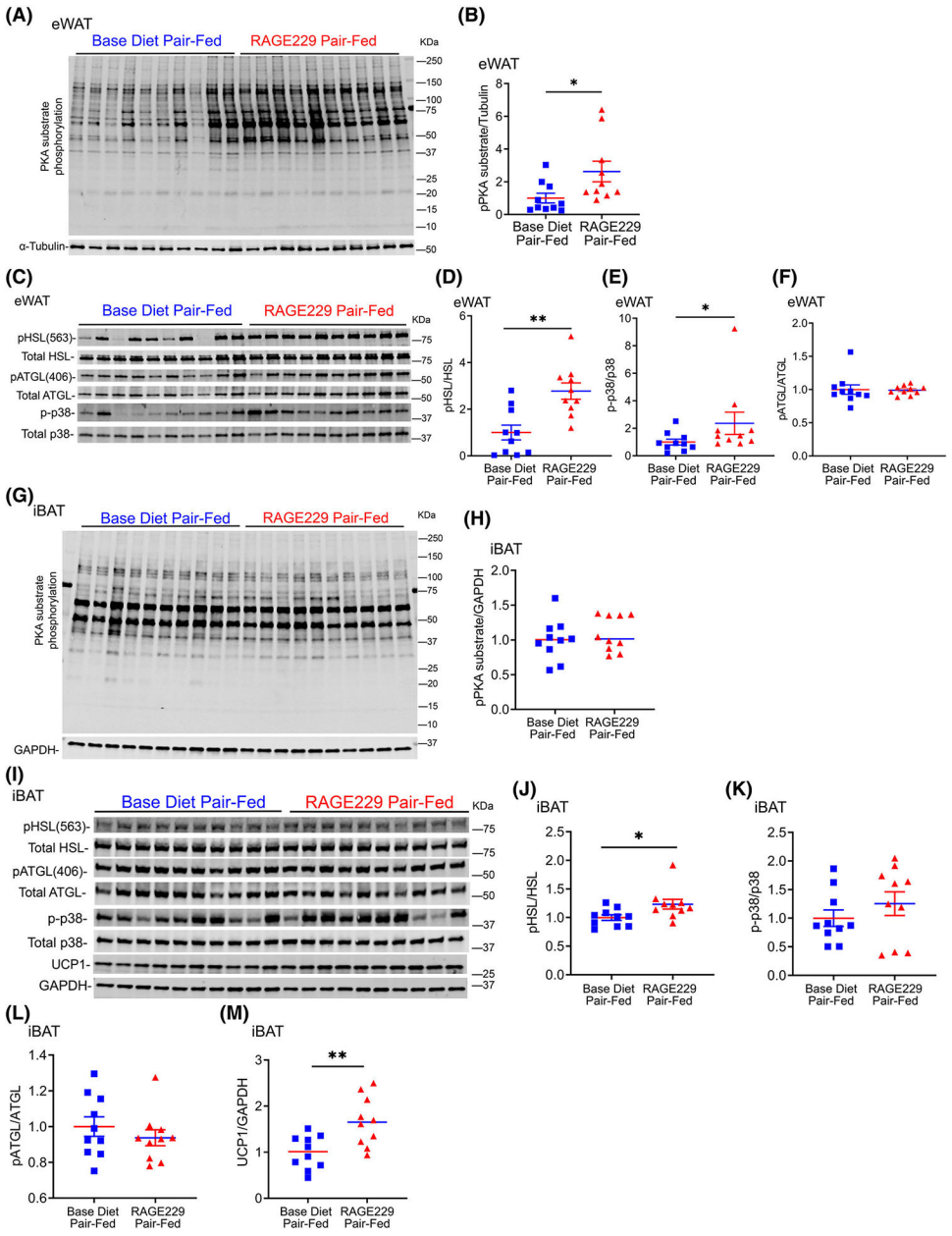

FIGURE 3.

Pair feeding of lean male mice with RAGE229–150 ppm diet results in higher PKA-dependent lipolytic and thermogenic markers in eWAT and iBAT depots compared with mice fed base diet. (A–F) Western blot analysis of eWAT lysate collected after 3 days of pair feeding probed for expression of PKA-substrate phosphorylation/α-tubulin, phosphorylated HSL-serine 563/total HSL, phosphorylated p38/total p38 MAPK, and phosphorylated ATGL-serine 406/total ATGL (n = 10 per group). (G–M) Western blot analysis of iBAT lysate collected after 3 days of pair feeding probed for expression of PKA-substrate phosphorylation/GAPDH, phosphorylated HSL-serine 563/total HSL, phosphorylated p38/total p38 MAPK, phosphorylated ATGL-serine 406/total ATGL, and UCP1/GAPDH (n = 10 per group). Tissues were collected from randomly fed mice. Data are presented as the

mean ± SEM. For group comparison, the Shapiro–Wilk normality test was conducted first for each group with prespecified significance level of 0.1, and if passed, the *t* test was implemented, whereas the nonparametric Wilcoxon rank sum test was used if normality was not established. eWAT, epididymal white adipose tissue; iBAT, interscapular brown adipose tissue; RAGE229, receptor for advanced glycation end products. *$p < 0.05$; **$p < 0.01$
[Color figure can be viewed at wileyonlinelibrary.com]

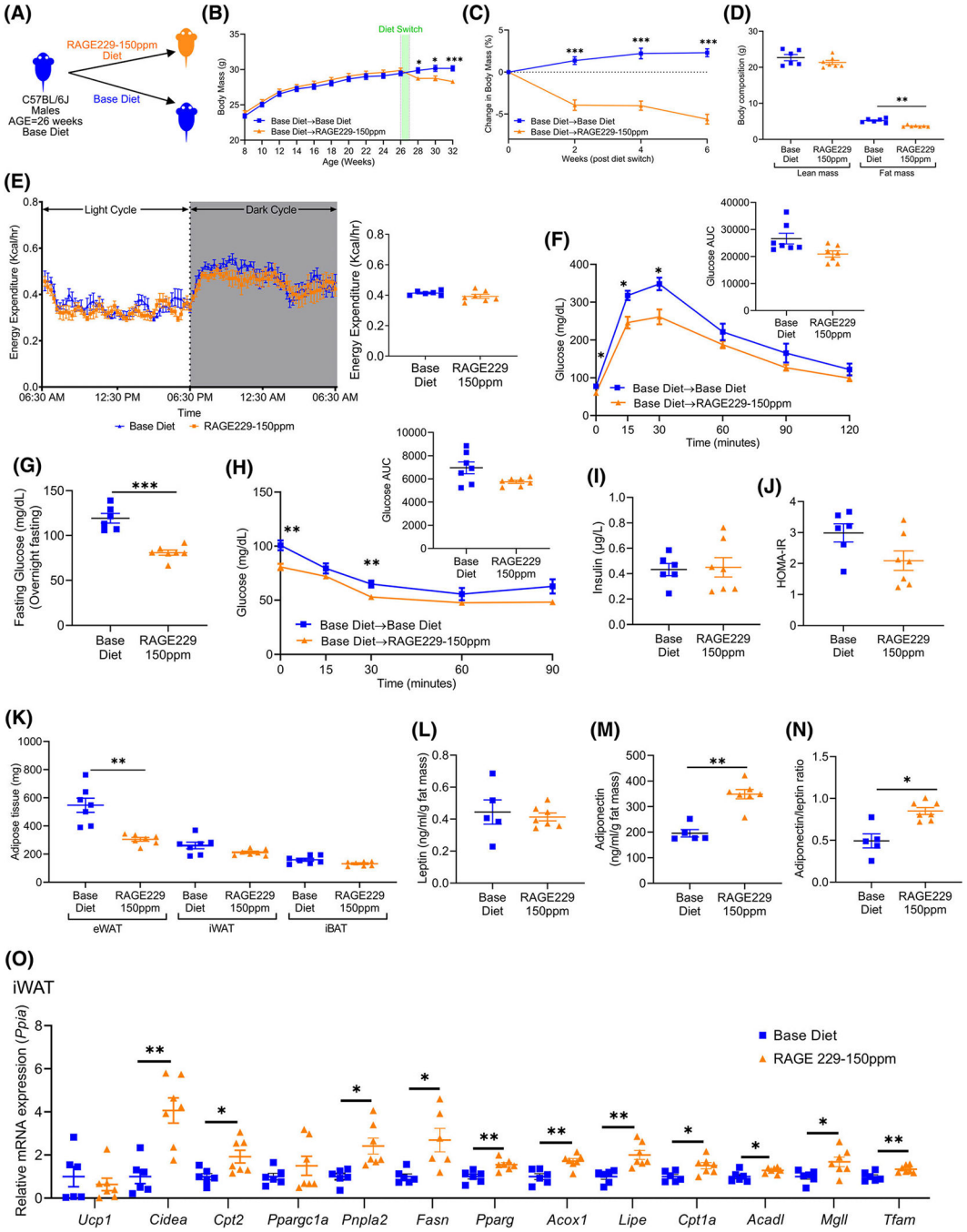

FIGURE 4.

Administration of RAGE229–150 ppm diet to lean male mice causes loss of body and fat mass and improves metabolic health. (A) Experimental schematic. (B) Body mass recorded over the indicated time course in mice fed base diet until age 26 weeks; mice then remained on base diet ($n = 24$) or were switched to RAGE229–150 ppm diet ($n = 27$). (C) Change in body mass (%) over 6 weeks after diet switch. (D) Lean mass and fat mass measured at 9 weeks after diet switch by DXA ($n = 6$ base diet, $n = 7$ RAGE229 diet). (E) Energy expenditure (light and dark cycle) measured at 10 weeks after diet switch ($n = 6$ base diet,

n = 7 RAGE229–150 ppm diet). (F) Post-overnight fasting glucose tolerance test at 6 weeks after diet switch (*n* = 7 per group). (G) Post-overnight fasting plasma glucose at 12 weeks after diet switch (*n* = 6 base diet, *n* = 7 RAGE229–150 ppm diet). (H) Post-6-hour fasting insulin tolerance test at 7 weeks after diet switch (*n* = 7 per group). (I,J) Post-overnight fasting plasma insulin and HOMA-IR at 12 weeks after diet switch (*n* = 6 base diet, *n* = 7 RAGE229–150 ppm diet). (K) Adipose tissue depot mass collected from randomly fed mice 12 weeks after diet switch (*n* = 7 per group). (L–N) Post-overnight fasting plasma leptin/fat mass, adiponectin/fat mass, and adiponectin/leptin ratio at 12 weeks after diet switch (*n* = 5 base diet, *n* = 7 RAGE229–150 ppm diet). (O) Relative expression of the indicated metabolic and thermogenic genes in iWAT collected from randomly fed mice (*n* = 6 base diet, *n* = 6–7 RAGE229–150 ppm diet) at 6 weeks after diet switch. Data are presented as the mean ± SEM. Data presented in panels B and C are combined from four independent cohorts. Multiple cohorts were employed for replication and in order to execute all of the biochemical, molecular, and physiological studies reported in this figure. For analysis of absolute body mass (panel B) over the indicated time period, piecewise linear mixed-effect model was fitted with node set at 26 weeks and difference was tested between the body mass of base diet and RAGE229–150 ppm diet groups after diet switch. A linear mixed-effect model was adopted for correlated/time-series data (B,C,E,F,H) with post hoc *t* test for group comparisons at each time point. For group comparison, the Shapiro–Wilk normality test was conducted first for each group with prespecified significance level of 0.1, and if passed, the *t* test was implemented whereas the nonparametric Kruskal-Wallis test/Wilcoxon rank sum test was used if normality was not established. AUC, area under the curve; DXA, dual-energy x-ray absorptiometry; HOMA-IR, homeostatic model assessment of insulin resistance; eWAT, epididymal white adipose tissue; iBAT, interscapular brown adipose tissue; iWAT, inguinal white adipose tissue; RAGE229, receptor for advanced glycation end products. *$p < 0.05$; **$p < 0.01$; ***$p < 0.001$ [Color figure can be viewed at wileyonlinelibrary.com]

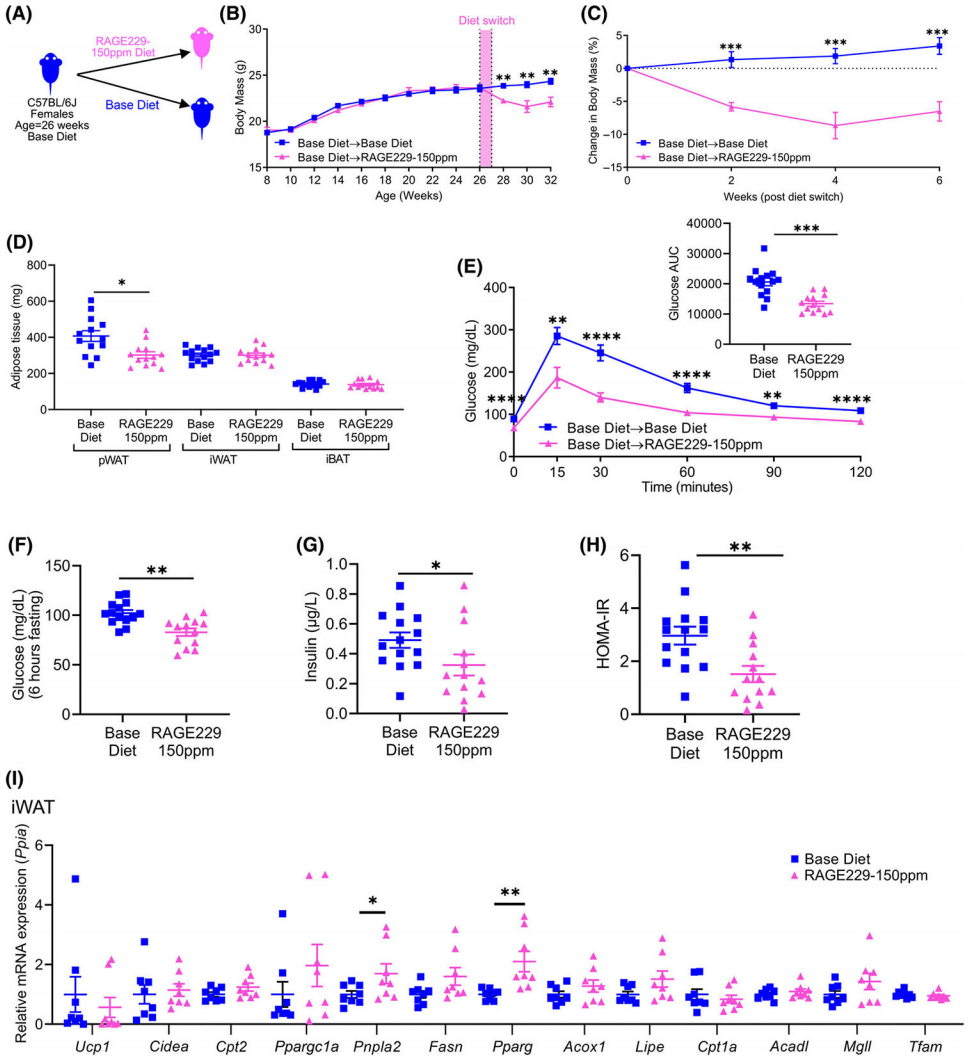

FIGURE 5.

Effects of RAGE229–150 ppm diet on body and fat mass and metabolic benefits are sex-independent: studies in female mice. (A) Experimental schematic. (B) Body mass recorded over the indicated time course in female lean mice fed base diet until age 26 weeks; mice then remained on base diet ($n = 14$) or were switched to RAGE229–150 ppm diet ($n = 13$) for 6 weeks. (C) Change in body mass (%) over 6 weeks after diet switch. (D) Adipose tissue depot mass ($n = 14$ base diet, $n = 13$ RAGE229–150 ppm diet) at 8 weeks after diet switch. (E) Post-6-hour fasting glucose tolerance test at 6 weeks after diet switch ($n = 14$ base diet, $n = 13$ RAGE229–150 ppm diet). (F–H) Post-6-hour fasting plasma glucose, insulin, and HOMA-IR at 8 weeks after diet switch ($n = 14$ base diet, $n = 13$ RAGE229–150 ppm diet). (I) Relative expression of indicated metabolic and thermogenic genes in iWAT collected from mice fasted for 6 hours ($n = 8$ per group) at 8 weeks after diet switch. Data are presented as the mean ± SEM. For analysis of absolute body mass (panel B) over the indicated time period, piecewise linear mixed-effect model was fitted, with node set at 26 weeks, and difference was tested between the body mass of the weight of base diet and RAGE229–150 ppm diet groups after diet switch. Linear

mixed-effect model was adopted for correlated/time-series data (B,C,E) with post hoc *t* test for group comparisons at each time point. For group comparison, the Shapiro–Wilk normality test was conducted first for each group, with prespecified significance level of 0.1, and if passed, the *t* test was implemented whereas the nonparametric Kruskal-Wallis test/Wilcoxon rank sum test was used if normality was not established. AUC, area under the curve; HOMA-IR, homeostatic model assessment of insulin resistance; iWAT, inguinal white adipose tissue; pWAT, perigonadal white adipose tissue; iBAT, interscapular brown adipose tissue; RAGE229, receptor for advanced glycation end products. *$p < 0.05$; **$p < 0.01$; ***$p < 0.001$; ****$p < 0.0001$ [Color figure can be viewed at wileyonlinelibrary.com]

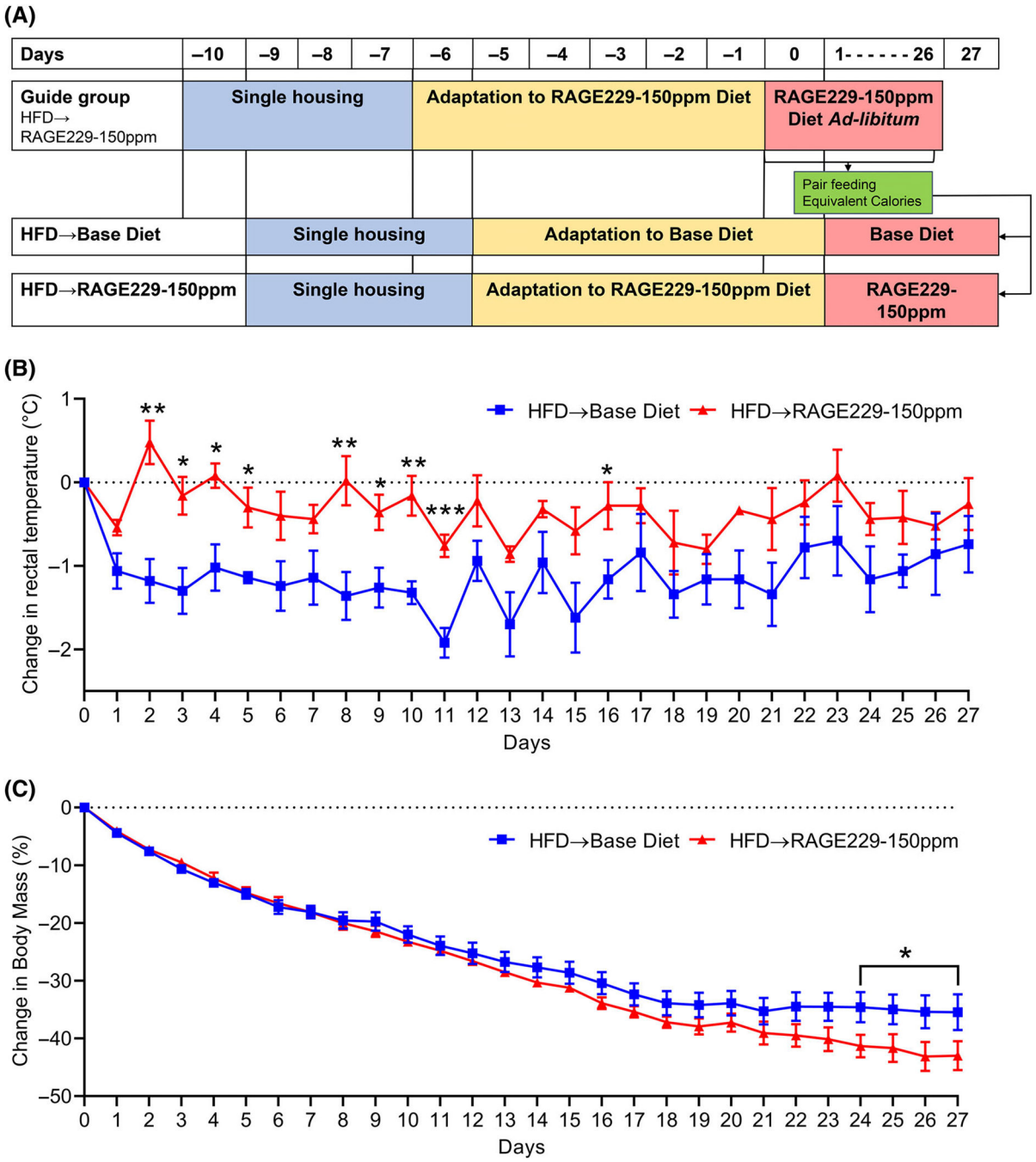

FIGURE 6.

Pair feeding RAGE229–150 ppm diet to obese mice undergoing diet-induced weight loss increases thermogenesis. (A) Experimental schematic of pair-feeding mice switched from HFD to RAGE229–150 ppm or base diet. (B) Change in daily rectal temperature measured over the indicated time course after diet switch in pair-fed mice ($n = 5$ per group). (C) Change in body mass measured over the indicated time course after diet switch in pair-fed mice ($n = 5$ per group). Linear mixed-effect model was adopted for correlated/time-series data, with post hoc t test for group comparisons at each time point. For change in body mass

in pair-fed mice (panel C), one tailed *t* test was used to compare groups at each time point. HFD, high-fat diet; RAGE229, receptor for advanced glycation end products. *$p < 0.05$; **$p < 0.01$; ***$p < 0.001$ [Color figure can be viewed at wileyonlinelibrary.com]

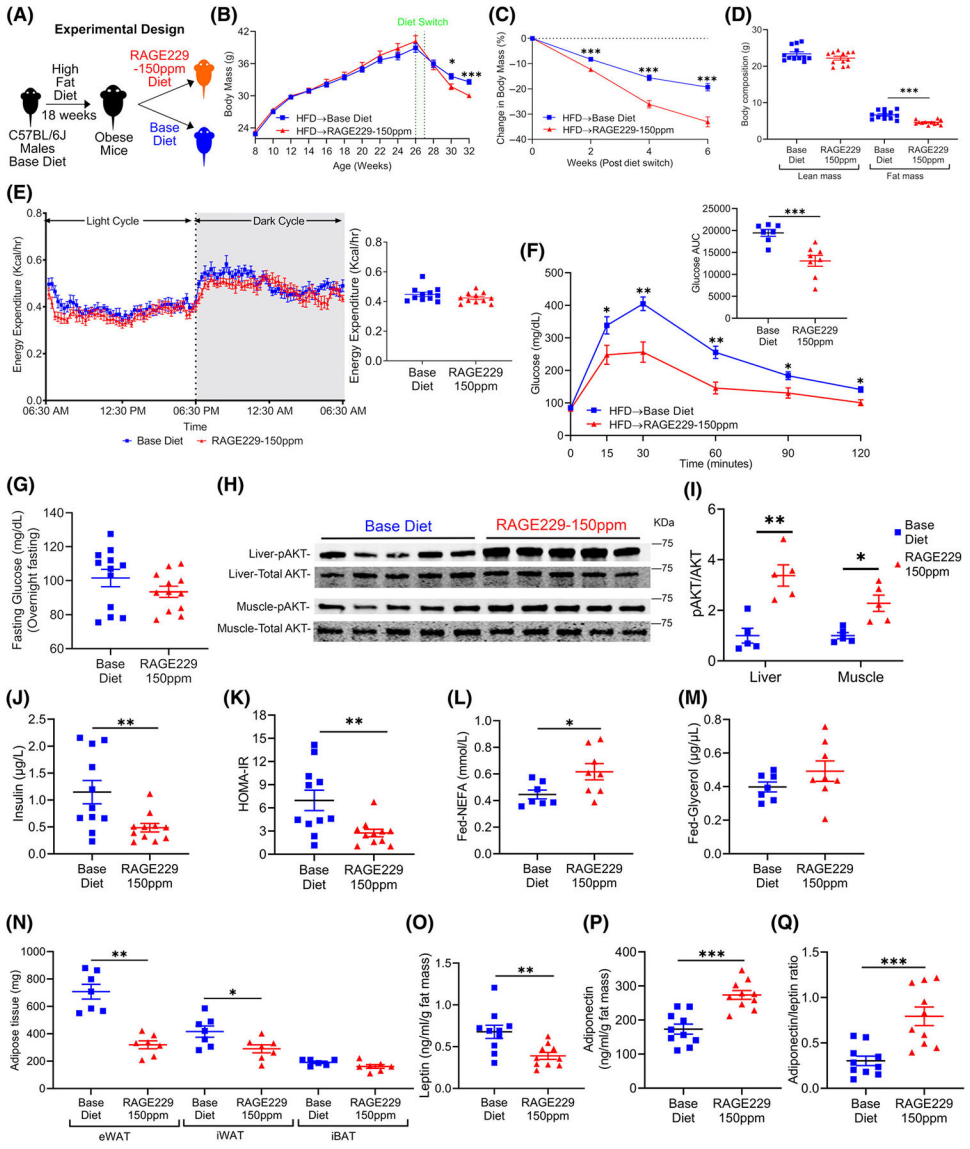

FIGURE 7.

Administration of RAGE229–150 ppm diet enhances loss of body mass and adiposity and improves metabolic health in male mice with established obesity undergoing weight loss. (A) Experimental schematic. (B) Body mass recorded over the indicated time course in male mice fed HFD between age 8 and 26 weeks to establish obesity; mice were then switched to base diet (n = 38) or RAGE229–150 ppm diet (*n* = 40). (C) Change in body mass (%) over 6 weeks after diet switch. (D) Lean mass and fat mass measured at 9 weeks after diet switch by DXA (*n* = 12 per group). (E) Energy expenditure of mice switched from HFD to base diet (*n* = 11) or RAGE229–150 ppm diet (*n* = 11) measured at 10 weeks after diet switch. (F) Post-overnight fasting glucose tolerance test in mice with obesity at 6 weeks after diet switch to either base diet (*n* = 7) or RAGE229–150 ppm diet (*n* = 8). (G) Post-overnight fasting plasma glucose (*n* = 12 per group) at 12 weeks after diet switch. (H,I) Western blot of liver and muscle tissue collected 15 minutes after intraperitoneal injection of insulin bolus and then probed for expression of phosphorylated Protein Kinase B AKT-serine 473/total

AKT (n = 5 per group). (J,K) Post-overnight fasting plasma insulin and HOMA-IR at 12 weeks after diet switch (n = 11 per group). (L,M) Randomly fed plasma NEFA and glycerol at 12 weeks after diet switch to either base diet (n = 7) or RAGE229–150 ppm diet (n = 8). (N) Adipose tissue depot mass collected from randomly fed mice 12 weeks after diet switch (n = 7 base diet, n = 6–7 RAGE229–150 ppm diet). (O–Q) Post-overnight fasting plasma leptin/fat mass, adiponectin/fat mass, and adiponectin/leptin ratio at 12 weeks after diet switch (n = 10 per group). Data are presented as the mean ± SEM. Data presented in panels B and C are combined from four independent cohorts. Multiple cohorts were employed for replication and in order to execute all of the biochemical, molecular, and physiological studies reported in this figure. For analysis of absolute body mass (panel B) over the indicated time period, piecewise linear mixed-effect model was fitted, with node set at 26 weeks, and difference was tested between the body mass of the weight of base diet and RAGE229–150 ppm diet groups after diet switch. Linear mixed-effect model was adopted for correlated/time-series data (B,C,F) with post hoc t test for group comparisons at each time point. For group comparison, the Shapiro–Wilk normality test was conducted first for each group, with prespecified significance level of 0.1, and if passed, the t test was implemented whereas the nonparametric Kruskal-Wallis test/Wilcoxon rank sum test was used if normality was not established. AUC, area under the curve; DXA, dual-energy x-ray absorptiometry; HFD, high-fat diet; HOMA-IR, homeostatic model assessment of insulin resistance; RAGE229, receptor for advanced glycation end products. *$p < 0.05$; **$p < 0.01$; ***$p < 0.001$ [Color figure can be viewed at wileyonlinelibrary.com]

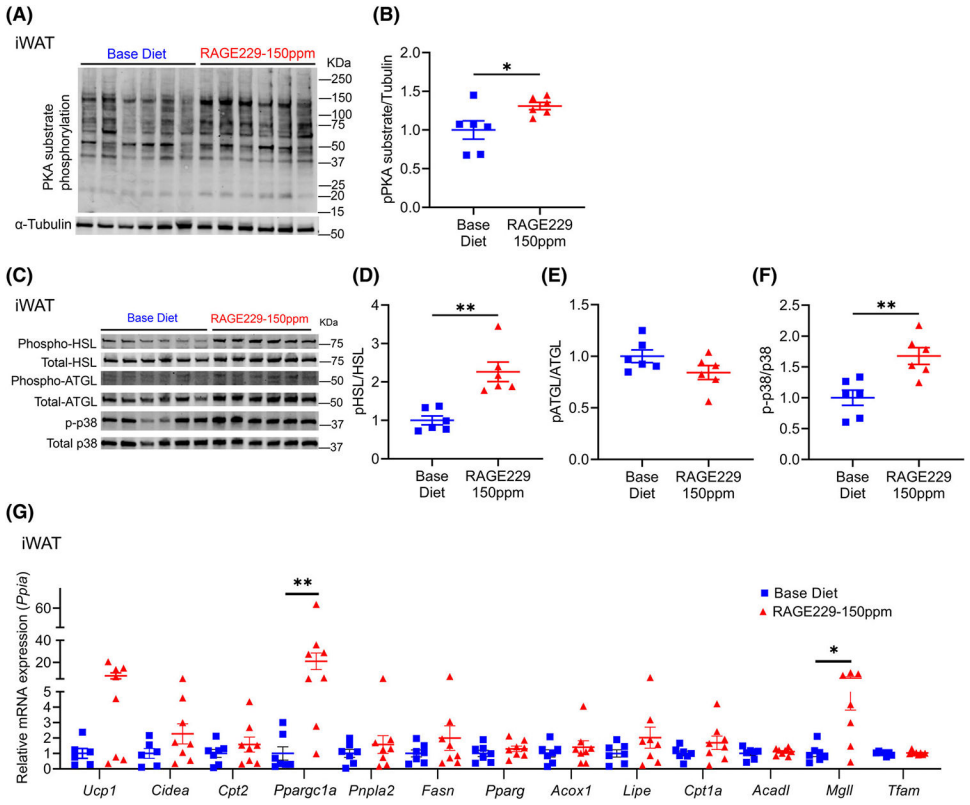

FIGURE 8.

Effect of RAGE229–150 ppm diet on molecular markers of lipolysis and lipid oxidation and thermogenic markers in iWAT depot of male mice with established obesity undergoing weight loss. (A–F) Western blot analysis of iWAT lysate probed for expression of PKA-substrate phosphorylation/α-tubulin, phosphorylated HSL-serine 563/total HSL, phosphorylated ATGL-serine 406/total ATGL, and phosphorylated p38/total p38 MAPK at 6 weeks after diet switch (n = 6 per group). (G) Relative expression of the indicated metabolic and thermogenic genes in iWAT collected at 6 weeks after diet switch (n = 6–7 base diet, n = 7–8 RAGE229–150 ppm diet). Tissues were collected from randomly fed mice. Data are presented as the mean ± SEM. For group comparison, the Shapiro–Wilk normality test was conducted first for each group, with prespecified significance level of 0.1, and if passed, the t test was implemented whereas the nonparametric Kruskal-Wallis test/Wilcoxon rank sum test was used if normality was not established. iWAT, inguinal white adipose tissue; RAGE229, receptor for advanced glycation end products. *$p < 0.05$; **$p < 0.01$ [Color figure can be viewed at wileyonlinelibrary.com]